DOI: 10.1002/ejic.200701216

Stepwise Spin Transition in a Mononuclear Iron(II) Complex with Unusually Wide Plateau

Birgit Weber,*[a] Chiara Carbonera,[b] Cedric Desplances,[b] and Jean-François Létard[b]

Dedicated to Professor Hanns-Peter Boehm on the occasion of his 80th birthday

Keywords: Iron / Magnetic properties / Spin crossover / Photomagnetism

The reaction of the Schiff-base like ligand H_2L [L^{2-} = (*E*,*E*)-({diethyl 2,2′-[1,2-phenylenebis(iminomethylidyne)]bis(3-oxobutanato)})] with iron(II) acetate in methanol in the presence of 4-cyanopyridine leads to the formation of an octahedral iron(II) complex with the formula $FeL(CNpy)_2 \cdot 0.25CNpy$ (**1**). The magnetic properties of this complex were investigated using temperature-dependent susceptibility measurements (SQUID) and Mössbauer spectroscopy. Both measurements indicate that the complex performs a stepwise spin transition with a large plateau in the region from 225 K to 125 K and $\gamma_{HS} \approx 0.25$. The molecule structure of the compound was determined at room temperature, 240 K ($\gamma_{HS} \approx 0.5$ according to susceptibility measurements) and 100 K. Two complex molecules were found in the asymmetric unit with strong π–π interactions between the phenylene rings of H_2L. In agreement with outcomes from the magnetic measurements, both iron centres are in the high-spin state at room temperature and in the low-spin state at 100 K. At 240 K one of the two iron centres is high-spin and the other one low-spin. The reason for the wide step with one fourth of the iron centres in the high-spin state is the additional distorted 4-cyanopyridine in the crystal that influences the transition temperature of the surrounding iron centres. The spin transition was followed in solution by using ^{1}H NMR spectroscopy. A gradual spin transition with $T_{1/2}$ = 238 K is obtained. Temperature-dependent diffuse reflectivity spectra show the occurrence of photoconversion at the surface of the sample but only about 6 % of the complex could be switched in bulk condition using a SQUID magnetometer and the stability of the photoinduced HS state with T_{LIESST} = 40 K is very weak.

1. Introduction

Spin-transition complexes (spin crossover, SCO) are an interesting class of compounds that can be switched on the molecular level between two or more states by the use of temperature, pressure or light.[1] The SCO bistability is one of the most promising for new electronic devices in molecular memories and switches as it may be controlled by different physical perturbations.[2] As part of a more general program we investigate the properties of mononuclear iron(II) complexes as possible building blocks for lager systems. Although octahedral iron(II) complexes are by far the most thoroughly investigated SCO complexes with the diamagnetic low-spin (LS) and the paramagnetic high-spin (HS) state,[1] there are only few examples for iron(II) based materials with stepwise spin transitions.[3,6–10] To date, three different possibilities are known in literature for describing stepwise spin transitions. One is related to binuclear complexes. Stepwise SCO are explained with the formation of [HS–HS], [HS–LS] and [LS–LS] spin pair states that could be directly monitored for example by Mössbauer spectroscopy and switched selectively by different wavelengths.[3] Results from DFT calculations agree with the conclusion of the phenomenological model, that the enthalpy of the [HS–LS] state must be lower than the average enthalpy of the [LS–LS] and the [HS–HS] states to create conditions for a two-step transition.[4] For mononuclear complexes with a unique crystallographic iron(II) site some kind of antiferrromagnetic interactions between the HS and the LS sublattices are made responsible for steps in the transition curve.[5] The two-step spin conversion of the N_4O_2 coordinated complex {Fe[5NO_2-sal-N(1,4,7,10)]} was successfully simulated using this model.[6] The third possibility to have a two-step spin transition is attributed to two different spin-crossover sites, each undergoing a transition at different temperatures.[1] One example is the compound $[Fe(btr)_3](ClO_4)_2$ (btr = 4,4′-bi-1,2,4-triazole) were two slightly different iron sites generate a two-step spin transition with a

[a] Ludwig Maximilian University Munich, Department of Chemistry and Biochemistry,
Butenandtstr. 5–13 (Haus F), 81377 München, Germany
Fax: +49-89-2180-77407
E-mail: bwmch@cup.uni-muenchen.de
[b] ICMCB, CNRS UPR No 9048 – Université Bordeaux 1, Groupe des Sciences Moléculaires,
87 Av. du Doc. A. Schweitzer, 33608 Pessac, France
Supporting information for this article is available on the WWW under http://www.eurjic.org or from the author.

approx. 25 K wide plateau.[7] Another example is the complex $[Fe(DPEA)(bim)](ClO_4)_2 \cdot 0.5H_2O$ (DPEA = (2-aminoethyl)bis(2-pyridylmethyl)amine, bim = 2,2-biimidazole) where the two steps are separated by an inflection point at 200 K.[8] The complex $[Fe(isoxazole)_6](BF_4)_2$ shows an incomplete two-step spin transition with about two-thirds of the iron(II) sites in the low-spin state at the plateau between 192 K and 91 K and a remaining high-spin molar fraction of 13% below 90 K. This behaviour is in agreement with the three molecules in the unit cell with two unique iron sites in a 1:2 ratio.[9] Other examples with independent iron sites coexisting in the same unit cell show incomplete spin conversions with one iron site remaining in the HS form.[10]

In this work we present a mononuclear spin-crossover complex with N_4O_2 coordination sphere that shows an unusually wide plateau at $\gamma_{HS} \approx 0.25$. Complexes of this type of equatorial Schiff base like ligands were first investigated by Jäger et al.[11] So far only one-step spin transitions were observed for this class of complexes.[11,12] The reason for the behaviour of the compound presented here are four inequivalent iron(II) sites in the crystal lattice with slightly different chemical surrounding due to an additional distorted 4-cyanopyridine molecule in combination with strong π–π interactions between two neighbouring molecules.

2. Results

H_2L has been synthesised as described in literature[14] and its reaction with iron(II) acetate in methanol in the presence of 4-cyanopyridine (CNpy) gives $(FeL(CNpy)_2 \cdot 0.25CNpy)$ (**1**) in good yield (Scheme 1). This complex was fully characterised by elemental analysis, IR, DTG and mass spectroscopy as well as X-ray diffraction at different temperatures. The IR spectrum shows a band at 1693 that can be assigned to ν(C=O) carbonyl stretching frequency of the ethoxy group of H_2L and at 2243 cm^{-1} that can be assigned to the ν(C≡N) stretching frequency of the CNpy. Both bands are not split indicating the absence of a hydrogen bond network. The difference temperature thermogravimetric analysis shows the loss of 2.25 4-CNpy. The magnetic properties were determined by *T*-dependent susceptibility measurements using a SQUID magnetometer at two different field strengths (2000 G and 5000 G) and Mössbauer spectroscopy.

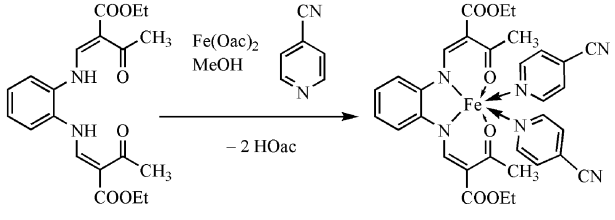

Scheme 1. Schematic representation of H_2L and synthetic route for the isolation of compound **1**.

2.1. Magnetic Properties

Figure 1 shows the temperature dependence of the magnetic properties of **1** (plot of the $\chi_M T$ product vs. *T*) analysed in the 5–350 K temperature range. The room temperature value of $\chi_M T = 2.76\ cm^3\,K\,mol^{-1}$ is characteristic of a complex essentially in the high-spin state and slightly smaller than the calculated spin-only value of $3.0\ cm^3\,K\,mol^{-1}$ expected for high-spin iron(II) ($S = 4/2$) with $g = 2$. The temperature was increased until at 350 K a plateau with $\chi_M T = 3.08\ cm^3\,K\,mol^{-1}$ is reached. As *T* is lowered, $\chi_M T$ decreases gradually. Around 240 K ($\chi_M T = 1.46\ cm^3\,K\,mol^{-1}$) an inflection point is observed followed by a small hysteresis (cooling $T_{1/2} = 232$ K and heating $T_{1/2} = 234$ K) that passes into a plateau in the region ≈ 225–125 K. The average value of $\chi_M T$ at the plateau is $0.77\ cm^3\,K\,mol^{-1}$ at 175 K. Below 125 K, $\chi_M T$ decreases again in a second more cooperative step with a small hysteresis (cooling $T_{1/2} = 109$ K and heating $T_{1/2} = 117$ K) and $\chi_M T = 0.07\ cm^3\,K\,mol^{-1}$ at 75 K. This behaviour indicates a two-step $S = 2 \Leftrightarrow S = 0$ spin conversion with about 75% of the iron(II) atoms in the first and about 25% in the second step.

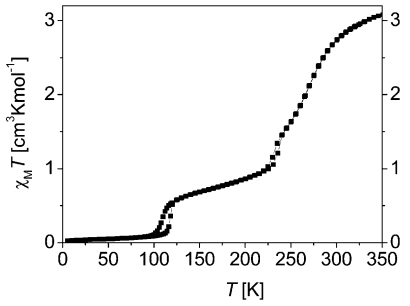

Figure 1. Plot of the $\chi_M T$ product vs. *T* for compound **1**.

The spin transition was also followed by using Mössbauer spectroscopy in the temperature region 80–270 K. Selected spectra at different temperatures are given in Figure 2 with the high-spin mol fraction (γ_{HS}) indicated. Values of the Mössbauer parameters obtained by least-squares fitting of the spectra are gathered in Table S1 in the Supporting Information. A plot of the half-width of the lines in the LS and the HS state as function of temperature is also given in Supporting Information (see Figure S1).

At 80 K the Mössbauer spectrum consists of a quadrupole split doublet with an isomer shift of 0.44 mm/s and a quadrupole splitting of 1.26 mm/s. These parameters are typical of iron(II) in the LS state. No evidence of a residual HS fraction is found. The line width of the doublet is with 0.33 mm/s broader than that found for similar iron(II) complexes.[12] Additionally the doublet is asymmetric. This is an indication of at least two iron centres with a slightly different chemical surrounding. Indeed, a much better agreement between the theoretical and the experimental data is obtained if two different low-spin iron(II) centres are taken into account and the line width for the two doublets is with

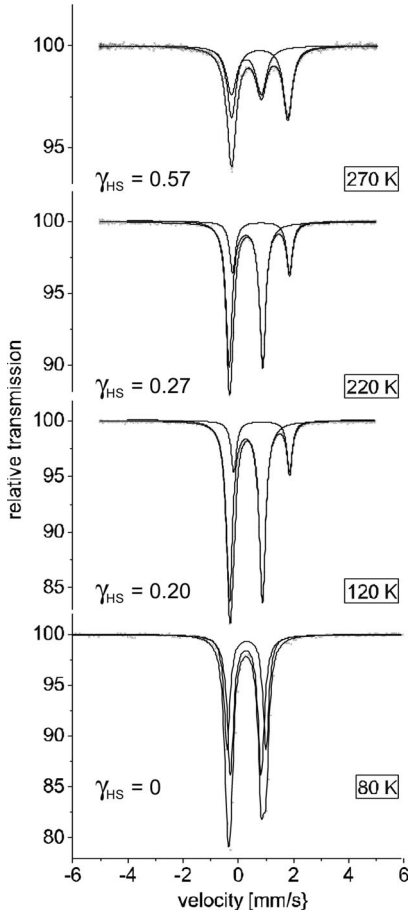

Figure 2. Plot of the Mössbauer spectra of compound 1 at 80, 120, 220 and 270 K with the high-spin molar fraction indicated.

0.25 mm/s and 0.28 mm/s, respectively, in the region found for similar iron(II) complexes.[12] At 110 K, the line width of the LS doublet decreases and an additional doublet with an isomer shift of 0.99 mm/s and a quadrupole splitting of 2.15 mm/s is observed. These parameters are characteristic of HS iron(II). The ratio of A_{HS}/A_{tot} is with 0.18 similar to the high-spin molar fraction value of about 0.2 obtained from the magnetic measurements. This ratio does not change significantly in the temperature region between 120 and 230 K. The average value of A_{HS}/A_{tot} at the plateau is 0.23. In the region of the plateau the line widths of the LS and the HS species are in the region of 0.27 and 0.23 mm/s and do not change significantly as a function of temperature. This is an indication that there are at least two iron centres that have a slightly different chemical surrounding. One possible reason for the stepwise spin transition with the large plateau is therefore the presence of two or more iron centres with slightly different chemical surrounding. Above 230 K the A_{HS}/A_{tot} ratio changes continuously in favour for the HS species. However, the line width of both doublets increases, which can be attributed to the increasing temperature and the lower resolution of the Mössbauer spectra.

2.2. X-ray Structure Analysis

An ORTEP view of **1** at 240 K as typical representative for the three different temperatures is shown in Figure 3. Selected bond lengths and angles are given in Table 1.

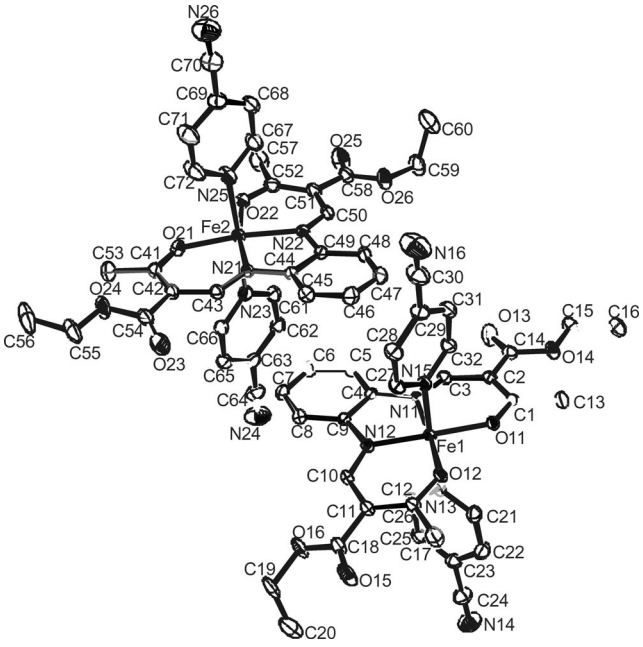

Figure 3. ORTEP drawing of the asymmetric unit of 1 at 240 K. Hydrogen atoms and solvent molecules were omitted for clarity. Thermal ellipsoids are shown at the 50% probability level.

Table 1. Selected bond lengths [Å] and angles [°] for 1 at room temp. 240 K and 100 K.

T [K]	S	Fe–N1/2	Fe–O1/2	Fe–N3/4	O1–Fe–O2	Nax–Fe–Nax	∠ L1, L2c
100	0, 0	1.895(2)	1.942(2)	1.979(2)			
		1.899(2)	1.947(2)	1.985(2)	90.23(6)	174.7(1)	80.1 / 7.7
		1.899(2)	1.933(2)	2.008(2)	89.89(6)	176.1(1)	
240	2, 0	1.909(2)	1.938(2)	2.009(2)			
		1.911(2)	1.944(1)	1.999(2)			
		1.911(2)	1.951(1)	2.007(2)	91.70(5)	174.4(1)	80.3 / 6.6;
		2.034(2)	1.967(2)	2.228(2)	102.74(6)	175.9(1)	77.3
		2.040(2)	1.973(2)	2.231(2)			
293	2, 2	2.061(2)	1.978(1)	2.289(2)			
		2.068(2)	1.982(1)	2.285(2)	105.39(6)	176.1(1)	77.6 / 7.7
		2.029(2)	1.970(1)	2.177(2)	103.61(6)	173.8(1)	
		2.037(2)	1.992(1)	2.238(2)			

As indicated by the results of Mössbauer spectroscopy, two or more complex molecules with slightly different chemical surrounding are expected in the asymmetric unit of the crystal. Indeed, two complex molecules and a disordered 4-CNpy molecule are found. The temperatures for X-ray structure analysis of the crystals were selected using the results form the magnetic measurements as guideline. They are room temperature for the pure HS compound, 100 K for the pure LS compound and 240 K for a 1:1 mixture of HS and LS complex. Attempts to solve the X-ray structure of the complex in the region of the plateau (225–125 K) did not meet with success, probably because the number of inequivalent iron centres in this temperature region increases and the quality of the data decreases.

Intramolecular changes during the spin transition: The average bond lengths of the iron centre in the high-spin state are 2.04 Å (Fe–N_{eq}), 1.98 Å (Fe–O_{eq}) and 2.24 Å (Fe–N_{ax}). Upon spin transition a shortening of the bond lengths of about 10% is observed, as discussed in the literature for other iron(II) spin crossover complexes. This shortening is more pronounced for the axial than for the equatorial ligands. The average distances in the low-spin state are 1.90 Å (Fe–N_{eq}), 1.94 Å (Fe–O_{eq}) and 2.00 Å (Fe–N_{ax}). A sensible tool for determining the spin state of this type of iron complexes is the O–Fe–O angle, the so-called bite of the ligand. It changes from an average of 104 in the high-spin state to 91° in the low-spin state. Taking this information, it is now possible, to follow the spin transition by X-ray structure analysis. The results agree very well with the results of magnetic measurements. At room temperature both molecules are in the high-spin state and at 100 K both molecules are in the low-spin state. At 240 K (γ_{HS} = 0.5 according to the magnetic measurements) one complex molecule in the asymmetric unit is in the low-spin state (Fe1) and the other molecule is in the high-spin state (Fe2).

The two phenylene rings of the equatorial ligand of the neighbouring molecules give rise to π–π interactions. Selected intermolecular C–C distances as well as the Fe···Fe distances between the two molecules within the asymmetric unit are reported in Table 2. Several contacts shorter than 3.6 Å (sum of the Van der Waals distances for C) are found, and a preferred 1:1 ordering of high-spin and low-spin molecules – similar to the HS–LS spin pairs in dinuclear complexes, might be one reason for the large plateau. This possibility can be ruled out as the plateau is at γ_{HS} = 0.25 and not at γ_{HS} = 0.5. Indeed, around 240 K the spin transition is rather abrupt and the π–π interactions appear to increase the cooperative interactions between the iron centres during the spin transition. Closer inspection reveals some more differences between the two iron centres that might influence the spin-transition temperature. One is the orientation of the axial ligands, which is coplanar for the one iron centre while for the other one (with the higher transition temperature) an angle of about 90° is enclosed. The second point is the additional CNpy in the crystal. Different distances between the pyridine nitrogen and the surrounding iron centres are observed. An extract of the molecule packing around the CNpy is given in Figure 4 and selected intermolecular distances are summarised in Table 3. As one CNpy is surrounded by four iron centres, this gives a good explanation for the plateau around $\gamma_{HS} \approx 0.25$ and the other small steps in the transition curve. At 240 K the iron centres in the LS state (Fe1a, Fe1b) are father away from the CNpy nitrogen than the iron centres that are still in the HS state (Fe2a, Fe2b). Obviously the iron centres in the immediate vicinity of the CNpy molecule have lower transition temperatures. However, only every second CNpy position is occupied and therefore only every second pair of Fe2 centres is in the influence sphere of a CNpy molecule. Thus one quarter of the complex molecules has a significantly lower transition temperature. In Figure 5 the interactions between the ethoxy group and the phenylene ring of neighbouring molecules in the crystal is displayed. Several C–C contacts shorter than 4.2 Å (sum of the Van der

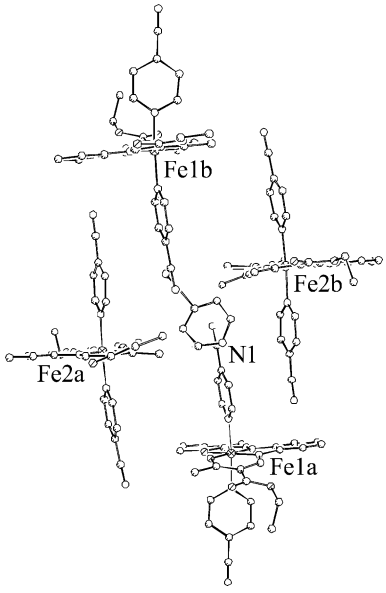

Figure 4. Packing of the molecules in the crystal around the CNpy molecule at 100 K.

Table 2. Selected intermolecular distances of 1 at room temp. 240 K and 100 K within the asymmetric unit.

	$T \approx 100$ K	$T \approx 240$ K	Room temp.
Fe1–Fe2	9.10	9.31	9.50
C4–C46	3.36	3.42	3.33
C4–C47	3.60	3.69	3.74
C5–C45	3.54	3.55	3.56
C5–C46	3.39	3.40	3.37
C5–C47	3.40	3.45	3.50
C5–C48	3.56	3.63	3.80
C6–C45	3.34	3.35	3.41
C7–C45	3.39	3.46	3.48

Table 3. Selected intermolecular distances of 1 at room temp. 240 K and 100 K.

	$T \approx 100$ K	$T \approx 240$ K	Room temp.
Fe1a–Fe1b	18.89	19.24	19.33
Fe2a–Fe2b	11.10	10.89	10.81
Fe1a–Fe2a	10.38	10.44	10.34
Fe1a–Fe2b	10.50	11.64	11.76
Fe1a–N1	8.32	8.62	8.76
Fe1b–N1	11.09	11.17	11.12
Fe2a–N1	6.55	6.31	6.25
Fe2b–N1	5.71	5.78	5.74
C13–C8′	3.63	3.69	3.64
C13–C9′	3.88	3.93	3.88
C15–C5′	3.82	3.89	3.92
C15–C6′	3.57	3.64	3.68
C15–C7′	3.95	4.00	3.96
C15–C8′	4.49	4.53	4.44
C16–C5′	3.57	3.61	3.93
C16–C6′	3.88	3.91	4.20

Waals distances for C and H and the distance of the C–H bond length) are found (Table 3). Nevertheless the spin transition is gradual until γ_{HS} = 0.5. Probably the ethoxy group is too flexible and therefore not suitable for transmitting cooperative interactions during the spin transition in the crystal. A similar observation was made for the same complex with pyridine as axial ligands.[11b] The increase of cooperative interactions during the spin transition of the second half of the molecules is probably due to the π–π interactions between the phenylene rings of the neighbouring molecules.

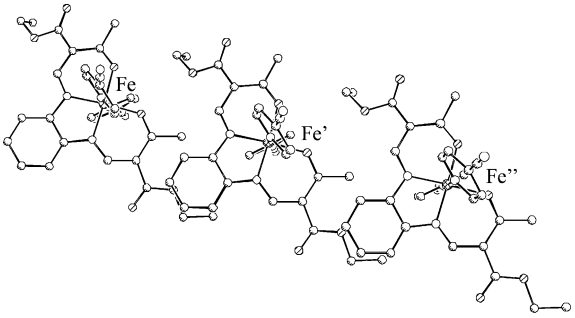

Figure 5. Packing of the molecules in the crystal.

2.3 Investigations in Solution Using ^{1}H NMR Spectroscopy

Variable temperature NMR spectroscopy is frequently used for investigating spin transitions in the solid state[21] or in solution (Evans Method).[22] We recently reported the possibility to follow a spin transition in solution by interpretation of the temperature dependence of the ^{1}H NMR chemical shifts of the compounds and by this eliminate the disadvantages of Evans Method.[23] In order to proof the influence of the additional CNpy molecule on the spin transition, **1** was dissolved in a 0.5 M solution of CNpy in [D_8]-toluene. The iron centre was assumed to retain its octahedral coordination sphere; however, the remaining CNpy molecules in solution are most likely to far from the iron centre away to influence its transition temperature. Steps introduced by interactions with the additional cyanopyridine in the solid and/or packing effects are expected to disappear. Figure 6 shows the ^{1}H NMR spectrum of **1** in a 0.5 M solution of CNpy in [D_8]toluene at 35 °C with the signal assignment to the right. The assignment was accomplished by spectral comparison with the previously published spectra[23] and by taking the different line widths and relative intensities into consideration. The position of the signals of the protons A, B, C and D with the relative intensities of 3 (A and B), 2 (C) and 1 (D) is comparable to those of the previously published complex with the same equatorial ligand in a pyridine/toluene mixture (50:50, v/v). The signals were therefore assigned to the CH_3 group (A) and the ethyl group (B, C) of the substituents of the equatorial ligand. The signal with a relative intensity of 1 was assigned to the proton D of the phenlyene ring. The signals of the two remaining protons were not assigned. Considering the NMR spectra of this type of complexes in pyridine,[23] the HC–N proton should be in the 400–500 ppm region of the spectrum but is very broad and therefore difficult to detect. The signal of second proton of the phenylene ring is probably in the –5–5 ppm region of the spectrum, but too broad to be detected because of additional signals from the solvent and impurities.

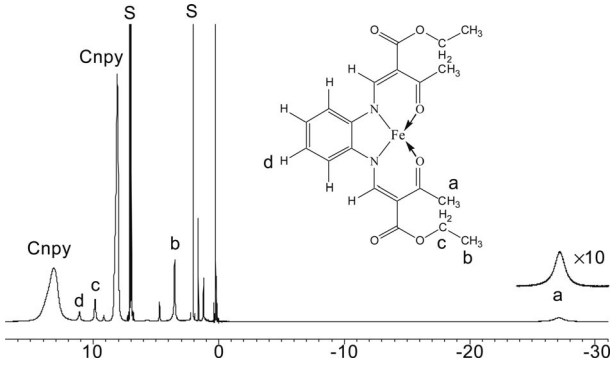

Figure 6. ^{1}H NMR spectrum of **1** in a 0.5 M solution of CNpy in toluene at 35 °C. The signal assignment is given at the right. S denotes the solvent toluene and CNpy denotes the 4-cyanopyridine.

The temperature dependence of the NMR parameters of **1** (isotropic shifts plotted vs. 1/*T*) is given in part A of Figure 7. Above 50 °C (323.15 K; 1/*T* = 3.1 1000/K) the behaviour is similar to those expected for pure HS complexes. At lower temperatures, the isotropic shifts move rapidly towards zero as reported previously for this type of spin-transition complexes with pyridine as axial ligands.[23] The

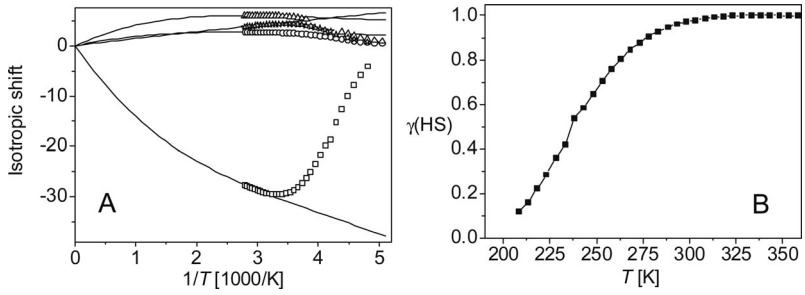

Figure 7. (A) Isotropic shifts of **1** plotted vs. 1/*T* (dots). The solid lines represent the calculated shifts of the pure HS complex using the extended Curie law [Equation 1]. The fitting parameters are given in the text. (B) HS mol fraction (γ_{HS}) of **1** obtained by interpretation of the isotropic shifts using the extended Curie law.

paramagnetic shift of the pure HS complex above 50 °C does not follow the ideal Curie law straight line. This is most probably due to thermally accessible excited states. The experimental data in Figure 7 (A) were fit by taking an extended Curie law into account with different Curie constants (or spin densities) for the ground and excited states, see Equation (1).

$$\delta_n^{con} = (F/T)\{W_1C_{n1}^2 + W_2C_{n2}^2e^{-\Delta E/kT}\}/\{W_1 + W_2e^{-\Delta E/kT}\} \quad (1)$$

W_1 and W_2 are the weighting factors for the ground and excited state [$S(S+1)$ in each case], C_{n1} and C_{n2} are the orbital coefficients (spin densities) for ground state and excited state, F is the Curie constant, ΔE is the energy difference between the ground state and the first excited state and k is the Boltzmann constant. Because the most likely excited state is that in which the formerly t_{2g} electrons are rearranged between the d_{xy} and d_{yz} orbitals, both the ground state and the first excited state were assumed to exhibit a total spin $S = 2$. Other possible spin states were also tried and shown not to produce reliable fits. The fit obtained with the TDF (temperature-dependent fitting) program written by Shokhirev and Walker[24] (solid lines) simulates the temperature dependence of the isotropic shift very well. The best-fit parameters are: $E_1(GS) = 2\ [(d_{xy})^2(d_{xz},d_{yz})^2(d_{z^2})^1(d_{x^2-y^2})^1]$, $E_1(ES) = 2\ [(d_{xy})^1(d_{xz},d_{yz})^3(d_{z^2})^1(d_{x^2-y^2})^1]$, $\Delta E_{1,2} = 402\ cm^{-1}$, MSD = 0.010, spin densities 1: –0.0108(a),0.0003(b), 0.0008(c), –0.0026(d); 2: –0.0466(a), 0.0082(b), 0.0176(c), –0.0036(d). The calculated isotropic shifts of the pure HS complex at lower temperature can now be used to determine the HS molar fraction (γ_{HS}) of the complex as function of temperature, see Equation (2).

$$\gamma_{HS} = [\delta^{con}(\text{measured})T]/[\delta^{con}(\text{calculated})T] \quad (2)$$

In part B of Figure 7 the average of the spin transition curves for the different protons is given. In Figure 8 γ_{HS} obtained in solution is compared with the results from SQUID measurements in the solid state. The $T_{1/2}$ in solution of 238 K is very similar to the $T_{1/2}$ of the first step in the solid state.

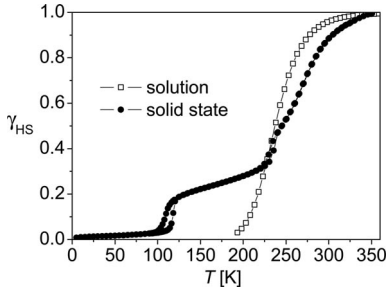

Figure 8. HS mol fraction (γ_{HS}) of **1** measured in solution (interpretation of the isotropic shifts; open squares) and in the solid state (SQUID measurements; dots •).

2.4 Optical and Photomagnetic Measurements

The thermal spin crossover of **1** was followed by measuring the diffuse absorption spectra (Figure 9). At room temperature, the absorption spectra are close to saturation what is in agreement with the dark colour of the compound due to strong MLCT transitions of the HS state. When the temperature is lowered to 80 K, a decrease of the absorption band around 850 nm, which is characteristic of the d-d transitions in the HS state, is observed. In the visible range that is linked to both, MLCT and d-d transitions of the LS state, no further increase of the absorption bands can be observed. This is most likely due to the already close saturation in the HS state. When the temperature is lowered further, the diffuse absorption spectrum recovers the shape and the intensity of the spectrum at 120 K; that is an increase of the d–d transition associated to the HS state at around 850 nm. An alternative way to follow the change of the diffuse absorption spectra as function of temperature is measuring the change of the reflectivity spectra at a selected wavelength. This is illustrated in Figure 10 for $\lambda = 881$ nm. Along the thermal HS→LS transition the intensity of the transition band at 881 nm decreases and consequently the reflectivity signal increases. For temperatures below 50 K the signal decreases again. These observations provide some evidence i) that at the surface the light-induced LS→HS conversion occurs according to the LIESST phenomenon,[25] and ii) that the lifetime of the photo-induced HS state below 50 K is sufficiently long to allow the optical excitation by a halogen light source delivering around 5 mW/cm^2. However, it must be noted that at 10 K not a complete recovery of the 280 K diffuse absorption spectrum did take place. According to Figure 10 only about 25% of the molecules (second step in the thermal spin transition) appear to be photo-converted. This might be due to the dark colour of the complex that prevents the light penetration into the sample and by this lead to an incomplete photo-excitation. Another possibility is that according to the inverse energy-gap law introduced by Hauser[26] or the T(LIESST) vs. $T_{1/2}$ relation of Létard,[27,28] only the second step in the thermal spin-transition curve is suitable for the generation of a photo-induced HS state with a sufficiently long lifetime.

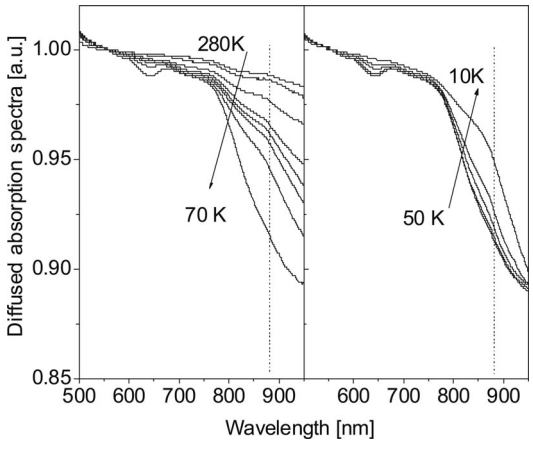

Figure 9. Dependency of the diffuse absorption spectra as function of both temperature and light-irradiation with (a) the thermal spin crossover and (b) the light-induced regions.

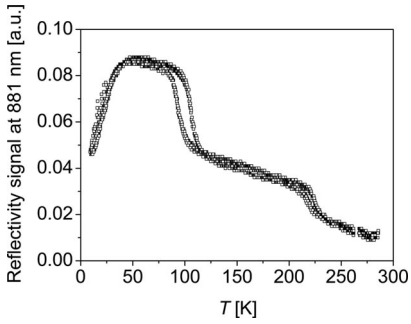

Figure 10. Dependency of the reflectivity signal at 881 nm as function of both temperature and light-irradiation.

In parallel the irradiation was also performed in bulk condition by i) using a Krypton laser emitting light at 647.1–676.4 nm or λ = 752.5–799.3 nm, ii) a photodiode-generated IR beam (λ = 830 nm). The application of the IR beam was not successful. The highest level of photo-induced HS state (6%) was obtained by the 752.5–799.3 nm irradiation (4% for irradiation at 647.1–676.4 nm). The plots of T(LIESST) experiments performed by irradiation both at 647.1–676.4 nm and at 752.5–799.3 nm are reported in Figure 11. In this procedure, the irradiation was maintained during several hours to assure the complete saturation of the signal, then the light was switched off and the temperature slightly increased at 0.3 K/min. The minimum of the $d\chi_M T/dT$ vs. T curve defines the T(LIESST) limit temperature (approximately 40 K for compound **1**) above which the light-induced HS state is no longer stable. Due to the very low amount of photo-excitation that can be ascribed to both, i) the high $T_{1/2}$ of the first step of the thermal spin transition and ii) the dark colour of the compound, no further photomagnetic experiments were performed, the determination of the kinetic parameters governing the relaxation process has not be performed.

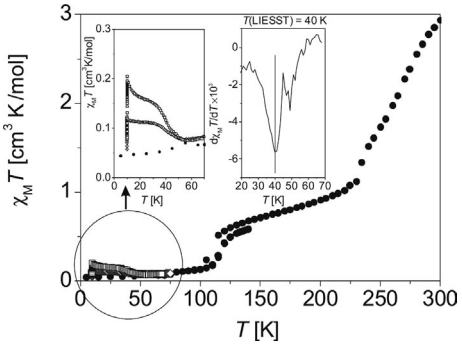

Figure 11. Temperature dependence of $\chi_M T$ for **1**. Bold dots • denote data recorded in the cooling and warming mode without irradiation; ✧ data recorded with irradiation at 10 K at 674.1–676.4 nm; T(LIESST) measurement: data recorded in the warming mode with the laser turned off after irradiation for one hour; □ data recorded with irradiation at 10 K at 752.5–799.3 nm; T(LIESST) measurement: data recorded in the warming mode with the laser turned off after irradiation for one hour.

3. Concluding Remarks

The synthesis and characterization of a new mononuclear SCO complex undergoing a stepwise spin transition is reported. In contrast to other stepwise spin-crossover compounds, the plateau at γ_{HS} = 0.25 cannot be directly correlated to the number of in-equivalent iron sites in the asymmetric unit. Reason for the significantly lower transition temperature of one fourth of the iron centers is an additional distorted 4-CNpyridine molecule in the crystal packing that has a noticeable short Fe–N distance to a quarter of the complex molecules. This observation is supported by Mössbauer spectroscopy. Here the line width of the LS duplet at 80 K is wider than expected and the doublet is asymmetric – two indications for two or more inequivalent iron sites. In the region of the plateau the line widths are smaller – one of the two iron sites is still in the LS state and the other one is in the HS state. Around 240 K (γ_{HS} = 0.5) an inflection point is observed in the magnetic measurements where the characteristic of the spin-transition changes from gradual to abrupt with small hysteresis. This behaviour can be explained with cooperative interactions between the phenylene rings of neighbouring molecules (π stacking). The coexistence of two different effects that influence the transition temperature (distorted additional 4-cynaopyridine) as well as the cooperative interactions during the spin transition (π stacking) are responsible for the complex structure of the transition curve. In solution a gradual spin transition with $T_{1/2}$ close to the first step in the transition curve of the solid sample is observed.

Due to the dark colour of the compound the measured reflectivity spectra were close to saturation. However, some indication for LIESST properties was detected. Of course, the level of photo-excitation in bulk condition was only of about 6% in the best condition by irradiating at 752.5–799.3 nm while at the surface the LS→HS photoconversion process was more evident. The stabilization of the photo-induced HS state in the complex **1**, with a T(LIESST) of about 40 K, appears to be very weak. This work confirms a recent study performed on other spin-crossover complexes belonging to the similar family,[12] involving this type of tetradentate ligand which possesses a degree of flexibility around the unsaturated nitrogen atoms connecting the aromatic phenyl rings and emphasizes the concept that vibrational aspects and hardness of the inner coordination sphere are the key factors for stabilizing the metastability of the light induced HS state.[27c,28b]

Experimental Section

General: All syntheses were carried out under argon using Schlenk tube techniques. Methanol was purified as described in the literature[13] and distilled under argon. The synthesis of the ligand H_2L[14] and iron(II) acetate[15] is described in literature. CNpy is commercially available and was used without further purification.

Physical Measurements: Magnetic measurements of pulverised samples were performed on a Quantum-Design-MPMSR-XL-SQUID-Magnetometer in a temperature range from 2 to 300 K.

All measurements were carried out at two field strengths (0.2 and 0.5 T) in the settle mode. The data were corrected for the magnetisation of the sample holder and diamagnetic corrections were estimated using Pascal's constants. Thermogravimetric analysis was performed on an electromagnetic-compensated thermobalance (home-made construction FSU Jena, Germany) with a heating rate of around 10 K/min. Elemental analysis was performed on an Elementar Vario EL instrument. Mössbauer spectra have been recorded using a conventional Mössbauer spectrometer operating in the constant acceleration mode. The sample was placed in an Oxford bath cryostat.

The NMR spectra were recorded on a JEOL EX 400e spectrometer operating at 400.182 MHz equipped with a variable-temperature unit over the temperature range – 85 to + 85 °C. [D_8]Toluene (99.6% D) was purchased from Euriso-top, degassed with argon and stored over molecular sieves. The NMR samples were prepared under argon using Schlenk techniques and locally-made sealing equipment. The concentration of the paramagnetic solute was in the range of 20 mg/mL. For the LIESST measurements, the measurement of the diffuse absorption spectra and reflectivity signal were performed by using a custom-built set-up equipped with a SM240 spectrometer (Opton Laser International). This equipment allows to record both the diffuse absorption spectra within the range of 500–900 nm at a given temperature and the temperature dependence (5–290 K) of the reflectivity signal at a selected wavelength (±2.5 nm). The diffuse reflectance spectrum was calibrated with respect to charcoal activated (Merck) as black standard and barium sulfate ($BaSO_4$, Din 5033, Merck) as white standard. The photomagnetic measurements were performed using a Spectra Physics Series 2025 Kr^+ laser (647.1–676.4 nm, 752.5–799.3 nm) or a diode laser (λ = 830 nm) coupled via an optical fibre to the cavity of the MPMS-55 Quantum Design SQUID-Magnetometer operating with an external magnetic field of 2 T within the 2–300 K temperature range and a speed of 10 K min^{-1} in the settle mode at atmospheric pressure.[16] The power of the laser beam on the sample whatever the selected wavelength(s) used was adjusted to 5 mW cm^{-2}. Bulk attenuation of light intensity was limited as much as possible by the preparation of a thin layer of compound. It is noteworthy that there was no change in the data due to sample heating upon laser irradiation. The weight of these thin-layer samples – approximately 0.2 mg – was obtained by comparison of the measured thermal spin-crossover curve with another curve of a more accurately weighed sample of the same compound. The data were corrected for the magnetisation of the sample holder and for diamagnetic contributions, estimated from Pascal's constants.

Crystal Structure Determinations: The intensity data for the compound **1** were collected on a Stoe IPDS diffractometer using graphite-monochromated Mo-K_α radiation. Data were corrected for Lorentz and polarisation effect and for absorption (XRed).[17] The structures were solved by direct methods (Sir 97)[18] and refined by full-matrix least-square techniques against F_o^2 (SHELXL-97).[19] The hydrogen atoms were included at calculated positions with fixed thermal parameters. All non-hydrogen atoms were refined anisotropically. Cell parameters and refinement results for all complexes are summarized in Table 4.[29] ORTEP-III was used for structure representation.[20]

$FeL(CNpy)_2$·0.25CNpy (1): H_2L (0.94 g, 2.41 mmol), iron(II) acetate (0.63 g, 3.61 mmol) and CNpy (5.5 g, 0.053 mol) were dissolved in methanol (35 mL) and refluxed for half an hour. After cooling, 5 mL of oxygen-free water was added. The solution was left standing for about 24 h at 5 °C to obtain black crystals. Yield 1.37 g (87%). $C_{20}H_{22}N_2O_6Fe(C_6H_4N_2)_{2.25}$ (676.5): C 57.98, H 4.79 N 13.96; found C 59.35, H 4.58, N 13.51. IR (Nujol): $\tilde{\nu}$ = 1693 ($\nu_{C=O}$), 2234 cm^{-1} ($\nu_{C=N}$). MS (DE): *m*/*z* 77 (100) [(4CNPy – HCN)$^+$], 104 (80) [4CNPy], 442 (15) [M$^+$]. DTG: weight change up to 150 °C: –5.8% due to loss of 4CNPy in the crystal (theory: 4.0% for 0.25 4-CNpy); up to 270 °C: –30.6% due to loss of two 4CNPy (theory: 31.9%); at 280 °C: decomposition.

Supporting Information (see also the footnote on the first page of this article): Least-squares-fitted Mössbauer data and a plot of the half-width of the Mössbauer lines of the HS and the LS form as function of temperature.

Table 4. Crystal data and structure refinement for **1** at room temperature, 240 K and 100 K.[29]

	Room temperature	240 K	100 K
Formula	$C_{33.5}H_{31}N_{6.5}O_6Fe$	$C_{33.5}H_{31}N_{6.5}O_6Fe$	$C_{33.5}H_{31}N_{6.5}O_6Fe$
M_r [g mol^{-1}]	676.492	676.492	676.492
Crystal system	triclinic	triclinic	triclinic
Space group	$P\bar{1}$	$P\bar{1}$	$P\bar{1}$
λ [Å]	0.71073	0.71073	0.71073
T [K]	293(3)	240(3)	105(3)
Crystal size [mm]	0.5 × 0.5 × 0.3	0.5 × 0.5 × 0.3	0.5 × 0.5 × 0.3
a [Å]	9.1660(7)	9.0968(7)	9.0395(9)
b [Å]	15.2030(12)	15.1155(12)	14.9708(15)
c [Å]	23.5030(17)	23.2588(16)	22.9009(19)
α [°]	87.557(9)	87.396(9)	87.536(11)
β [°]	86.464(9)	85.654(9)	85.162(11)
γ [°]	83.448(9)	84.075(9)	84.473(12)
V [Å^3]	3245.5(4)	3169.6(4)	3072(2)
Z	2	2	2
$d_{calcd.}$ [g cm^{-1}]	1.384	1.418	1.463
μ [mm^{-1}]	0.520	0.532	0.549
Absorption correction	X-red	X-red	X-red
Reflections collected	28124	27231	21963
Independent reflections (R_{int})	14337 (0.0487)	13889 (0.0544)	11751 (0.0446)
Data/restrains/parameters	14337/0/898	13889/0/948	11751/0/892
Final R indices [$I > 2\sigma(I)$]	R_1 = 0.0417, wR_2 = 0.1018	R_1 = 0.0413, wR_2 = 0.1000	R_1 = 0.0370, wR_2 = 0.0928
R indices (all data)	R_1 = 0.0703, wR_2 = 0.1111	R_1 = 0.0679, wR_2 = 0.1092	R_1 = 0.0559, wR_2 = 0.0989
GooF	0.911	0.920	0.981

Acknowledgments

This work has been supported financially by the Deutsche Forschungsgemeinschaft (DFG) (SPP 1137) and the Fonds der Chemischen Industrie. The authors would like also to thank the Aquitaine Region for funding the Photomagnetic platform at the ICMCB. B. W. would like to thank K. Achterhold and F. Parak for the acquisition of the Mössbauer spectra and S. R. Rill for the preparation of the NMR sample.

[1] a) H. A. Goodwin, *Coord. Chem. Rev.* **1976**, *18*, 293; b) P. Gütlich, *Struct. Bonding (Berlin)* **1981**, *44*, 83; c) E. König, *Prog. Inorg. Chem.* **1987**, *35*, 527; d) P. Gütlich, A. Hauser, *Coord. Chem. Rev.* **1990**, *97*, 1; e) E. König, *Struct. Bonding (Berlin)* **1991**, *76*, 51; f) P. Gütlich, A. Hauser, H. Spiering, *Angew. Chem. Int. Ed. Engl.* **1994**, *33*, 2024, and references cited therein; g) P. Gütlich, J. Jung, H. Goodwin, *Molecular Magnetism: From Molecular Assemblies to the Devices* (Eds.: E. Coronado, P. Delhaes, D. Gatteschi, J. S. Miller), NATO ASI Series E: Applied Sciences; Kluwer Academic Publishing, **1996**, vol. 321, p. 327; h) *Spin Crossover in Transition Metal Compounds, I–III*, *Topics in Current Chemistry* (Eds.: P. Gütlich, H. A. Goodwin), Springer-Verlag, Berlin, Heidelberg, New York, **2004**; i) J. A. Real, A. B. Gaspar, M. C. Munoz, *Dalton Trans.* **2005**, 2062; j) O. Sato, J. Tao, Y.-Z. Zhang, *Angew. Chem.* **2007**, *119*, 2200; *Angew. Chem. Int. Ed.* **2007**, *46*, 2152–2187.

[2] a) O. Kahn, C. Jay Martinez, *Science* **1998**, *279*, 44–48; b) O. Kahn, C. Jay, J. Kröber, R. Claude, F. Grolière, *Patent* **1995** EP0666561; c) J.-F. Létard, O. Nguyen, N. Daro, *Patent* **2005** FR0512476; d) J.-F. Létard, P. Guionneau, L. Goux-Capes, *Topics in Current Chemistry* (Eds.: P. Gütlich, H. A. Goodwin), Springer, Wien, New York, **2004**, *235*, 221.

[3] a) J. A. Real, H. Bolvin, A. Bousseksou, A. Dworkin, O. Kahn, F. Varret, J. Zarembowitch, *J. Am. Chem. Soc.* **1992**, *114*, 4650–4658; b) J. A. Real, I. Castro, A. Bousseksou, M. Verdaguer, R. Burriel, M. Castro, J. Linares, F. Varret, *Inorg. Chem.* **1997**, *36*, 455–464; c) J.-F. Létard, J. A. Real, N. Moliner, A. B. Gaspar, L. Capes, O. Cador, O. Kahn, *J. Am. Chem. Soc.* **1999**, *121*, 10630; d) G. Chastanet, A. B. Gaspar, J. A. Real, J.-F. Létard, *Chem. Commun.* **2001**, 819; e) G. Chastanet, C. Carbonera, C. Mingotaud, J.-F. Létard, *J. Mater. Chem.* **2004**, *14*, 3516–3523; f) V. Ksenofontov, H. Spiering, S. Reiman, Y. Garcia, A. B. Gaspar, N. Moliner, J. A. Real, P. Gütlich, *Chem. Phys. Lett.* **2001**, *348*, 381–386; g) V. Ksenofontov, A. B. Gaspar, V. Niel, S. Reiman, J. A. Real, P. Gütlich, *Chem. Eur. J.* **2004**, *10*, 1291–1298; h) J. A. Real, A. B. Gaspar, M. C. Munoz, P. Gütlich, V. Ksenofontov, H. Spiering, *Topics in Current Chemistry* (Eds.: P. Gütlich, H. A. Goodwin), Springer, Wien, New York, **2004**, *233*, 167; i) A. B. Gaspar, M. C. Munoz, J. A. Real, *J. Mater. Chem.* **2006**, *16*, 2522–2533; j) A. Bousseksou, G. Molnar, J. A. Real, K. Tanaka, *Coord. Chem. Rev.* **2007**, *251*, 1822–1833.

[4] S. Zein, S. A. Borshch, *J. Am. Chem. Soc.* **2005**, *127*, 16197–16201.

[5] a) M. Mikami, M. Konno, Y. Saito, *Chem. Phys. Lett.* **1979**, *63*, 566–569; b) N. Sasaki, T. Kambara, *Phys. Rev. B* **1989**, *40*, 2442; c) A. Bousseksou, J. Nasser, J. Linares, K. Boukheddaden, F. Varret, *J. Phys. I* **1992**, *2*, 1381; d) H. Spiering, T. Kohlhaas, H. Romstedt, A. Hauser, C. Bruns-Yilmaz, P. Gütlich, *Coord. Chem. Rev.* **1999**, *190–192*, 629–647.

[6] a) V. Petrouleas, J.-P. Tuchagues, *Chem. Phys. Lett.* **1987**, *137*, 21–25; b) D. Boinnard, A. Bousseksou, A. Dworkin, J.-M. Savariault, F. Varret, J.-P. Tuchaugues, *Inorg. Chem.* **1994**, *33*, 271–281.

[7] Y. Garcia, O. Kahn, L. Rabardel, B. Chansou, L. Salmon, J.-P. Tuchagues, *Inorg. Chem.* **1999**, *38*, 4663–4670.

[8] G. S. Matouzenko, J.-F. Letard, S. Lecocq, A. Bousseksou, L. Capes, L. Salmon, M. Perrin, O. Kahn, A. Collet, *Eur. J. Inorg. Chem.* **2001**, 2935–2945.

[9] W. Hibbs, P. J. van Koningsbruggen, A. M. Arif, W. W. Shum, J. S. Miller, *Inorg. Chem.* **2003**, *42*, 5645–5653.

[10] a) P. Poganiuch, S. Decurtins, P. Gütlich, *J. Am. Chem. Soc.* **1990**, *112*, 3270–3278; b) L. Wiehl, *Acta Crystallogr., Sect. B* **1993**, *49*, 289–303; c) R. Hinek, H. Spiering, D. Schollmeyer, P. Gütlich, A. Hauser, *Chem. Eur. J.* **1996**, *2*, 1427–1434.

[11] a) E.-G. Jäger, *Chemistry at the Beginning of the Third Millenium*, edited by L. Fabbrizzi, A. Poggi, Springer-Verlag, Heidelberg, **2000**, 103–138; b) G. Leibeling, Ph. D. Thesis, Universiy of Jena/Germany, **2003**; c) B. R. Müller, G. Leibeling, E.-G. Jäger, *Chem. Phys. Lett.* **2000**, *319*, 368–374.

[12] B. Weber, E. Kaps, J. Weigand, C. Carbonera, J.-F. Letard, K. Achterhold, F.-G. Parak, *Inorg. Chem.* **2008**, *47*, 487–496.

[13] Autorenkollektiv: *Organikum*, Johann Ambrosius Barth Verlagsgesellschaft mbH, Leipzig, **1993**.

[14] L. Wolf, E.-G. Jäger, *Z. Anorg. Allg. Chem.* **1966**, *346*, 76.

[15] B. Heyn, B. Hipler, G. Kreisel, H. Schreer, D. Walter, *Anorganische Synthesechemie*, Springer-Verlag, Heidelberg, **1986**, 2nd ed.

[16] a) J.-F. Létard, P. Guionneau, L. Rabardel, J. A. K. Howard, A. E. Goeta, D. Chasseau, O. Kahn, *Inorg. Chem.* **1998**, *37*, 4432–4441; b) J.-F. Létard, G. Chastanet, O. Nguyen, S. Marcen, M. Marchivie, P. Guionneau, D. Chasseau, P. Gütlich, *Monatsh. Chem.* **2003**, *134*, 165–182; c) J.-F. Létard, *J. Mater. Chem.* **2006**, *16*, 2550.

[17] G. M. Sheldrick, *SHELXL 97*, University of Göttingen, Germany, **1993**.

[18] A. Altomare, M. C. Burla, G. M. Camalli, G. Cascarano, C. Giacovazzo, A. Guagliardi, A. G. G. Moliterni, G. Polidori, R. Spagna, *SIR 97*, Campus Universitario Bari, **1997**; A. Altomare, M. C. Burla, G. M. Camalli, G. Cascarano, C. Giacovazzo, A. Guagliardi, A. G. G. Moliterni, G. Polidori, R. Spagna, *J. Appl. Crystallogr.* **1999**, *32*, 115–119.

[19] G. M. Sheldrick, *Acta Crystallogr., Sect. A* **1990**, *46*, 467–473.

[20] C. K. Johnson, M. N. Burnett, *ORTEP-III*, Oak-Ridge National Laboratory, Oak-Ridge, **1996**; L. J. Farrugia, *J. Appl. Crystallogr.* **1997**, *30*, 565.

[21] a) B. Maiti, B. R. McGarvey, P. S. Rao, L. C. Stubbs, *J. Magn. Res.* **1983**, *54*, 99–110; b) P. S. Rao, P. Ganguli, B. R. McGarvey, *Inorg. Chem.* **1981**, *20*, 3682–3688.

[22] a) K. F. Purcell, J. P. Zapata, *J. Chem. Soc. Chem. Commun.* **1978**, 497–499; b) J. K. Beattie, R. A. Binstead, R. J. West, *J. Am. Chem. Soc.* **1978**, *100*, 3044; c) R. A. Binstead, J. K. Beattie, E. V. Dose, M. F. Tweedle, L. J. Wilson, *J. Am. Chem. Soc.* **1978**, *100*, 5609–5614.

[23] B. Weber, F. A. Walker, *Inorg. Chem.* **2007**, *46*, 6794–6803.

[24] N. V. Shokhirev, F. A. Walker, *Temperature-Dependent Fitting*, http://www.shokhirev.com/nikolai/programs/prgsciedu.html.

[25] a) J. McGarvey, I. Lawthers, *J. Chem. Soc. Chem. Commun.* **1982**, 906; b) S. Decurtins, P. Gütlich, C. P. Köhler, H. Spiering, A. Hauser, *Chem. Phys. Lett.* **1984**, *105*, 1; c) S. Decurtins, P. Gütlich, K. M. Hasselbach, A. Hauser, H. Spiering, *Inorg. Chem.* **1985**, *24*, 2174; d) A. Hauser, *Chem. Phys. Lett.* **1986**, *124*, 543.

[26] a) A. Hauser, *Coord. Chem. Rev.* **1991**, *111*, 275; b) A. Hauser, J. Jeftic, H. Romstedt, R. Hinek, H. Spiering, *Coord. Chem. Rev.* **1999**, *190–192*, 471.

[27] a) J. F. Létard, P. Guionneau, L. Rabardel, J. A. K. Howard, A. E. Goeta, D. Chasseau, O. Kahn, *Inorg. Chem.* **1998**, *37*, 4432–4441; b) J.-F. Létard, G. Chastanet, O. Nguyen, S. Marcen, M. Marchivie, P. Guionneau, D. Chasseau, P. Gütlich, *Monatsh. Chem.* **2003**, *134*, 165–182; c) J.-F. Létard, *J. Mater. Chem.* **2006**, *16*, 2550.

[28] a) J.-F. Létard, L. Capes, G. Chastanet, N. Moliner, S. Létard, J. A. Real, O. Kahn, *Chem. Phys. Lett.* **1999**, *313*, 115; b) S. Marcen, L. Lecren, L. Capes, H. A. Goodwin, J.-F. Létard, *Chem. Phys. Lett.* **2002**, *358*, 87; c) J.-F. Létard, P. Guionneau,

O. Nguyen, J. S. Costa, S. Marcén, G. Chastanet, M. Marchivie, L. Capes, *Chem. Eur. J.* **2005**, *11*, 4582.
[29] CCDC-664970 (for **1** at room temp.), -664971 (for **1** at 240 K), and -664972 (for **1** at 100 K) contain the supplementary crystallographic data for this paper. These data can be obtained free of charge from The Cambridge Crystallographic Data Centre via www.ccdc.cam.ac.uk/data_request/cif.

Received: November 12, 2007
Published Online: February 13, 2008

